Equivalent Viscous Damping in Steel Structures Equipped With Dampers

Seyed Behdad Alehojjat [a], Omid Bahar [b,*], Masood Yakhchalian [a]

[a] *Department of Civil Engineering, Qazvin Branch, Islamic Azad University, Qazvin, Iran*

[b] *Structural Engineering Research Center, International Institute of Earthquake Engineering & Seismology (IIEES), Tehran, Iran*

Abstract

Determination of equivalent viscous damping (EVD) is an important step in the direct displacement-based design (DDBD) method. This study aims to investigate whether the proposed method used in the equivalent lateral force (ELF) procedure, according to ASCE/SEI 7, for the calculation of effective damping in steel structures equipped with fluid viscous dampers (FVDs) can be used in the DDBD method. In order to evaluate the accuracy of this method, modified Jacobsen's method and the approach used in Pennucci et al.'s study are applied to determine the EVD. At first, a set of steel structures with different heights and bays are designed for 0.75, 0.85 and 1.0 of the design base shears based on the primary calculation of the ELF procedure and then nonlinear time history analyses are carried out to determine the dampers constants and the EVD at two seismic hazard levels, i.e., design earthquake (DE) and maximum considered earthquake (MCE). According to the obtained results for the EVD, it is found that the obtained results in the ELF procedure has acceptably matched with Pennucci et al.'s approach. On the other hand, there are some differences between the obtained results and those obtained from modified Jacobsen's method. Therefore, the ELF proposed equation for calculating EVD can be used in the DDBD method in mid-rise steel structures equipped with FVDs to accurately determine the EVD.

Keywords: equivalent lateral force procedure, equivalent viscous damping, fluid viscous damper, direct displacement-based design.

1. Introduction

Direct displacement-based design (DDBD) as a simple and practical method has been widely developed since 1993 in the field of performance-based design. In the performance-based earthquake engineering framework, there are some procedures for designing, seismic evaluation, analysis of structures consisting ground motion record selection, etc. [1]. In the DDBD method, structures are designed by defining an inter-story drift ratio (IDR) value as a performance level for the specific level of seismic hazard level. The fundamental of the DDBD method is to convert a multi-degree of freedom (MDOF) structure to an equivalent single degree of freedom (SDOF) structure. The concept of the equivalent structure was firstly introduced by Gulkan and sozen [2] and then was developed by Shibata and Sozen [3]. Determining the equivalent viscous damping (EVD) of the equivalent SDOF structure has an important role in DDBD. In the past, the EVD was generally estimated by Jacobsen's

method [4, 5] via sinusoidal excitations based on initial stiffness. In the mentioned approach, the EVD was obtained by equating the energy absorbed by the hysteretic steady-state cyclic response at a given displacement level as:
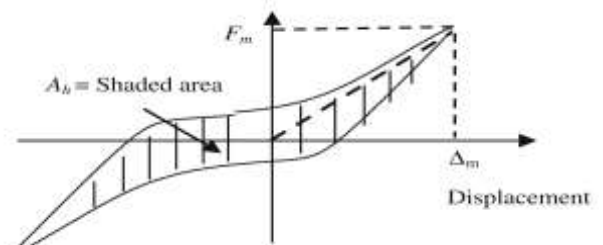
$$\xi_{hyst} = \frac{A_h}{2\pi F_m \Delta_m} \tag{1}$$

Fig. 1. Hysteresis curve for the EVD calculation [6]

*Corresponding Author: Email Address: omidbahar@iiees.ac.ir

where A_h is the area of a complete loop of hysteresis response and F_m and Δ_m are the maximum force and the displacement occurred in the complete cycle respectively. The graphical representation of the parameters was shown in Fig. 1. Latter, Rosenblueth and Herrera [7] modified Jacobsen's method by applying secant stiffness instead of initial stiffness. Jacobsen's damping secant stiffness is adopted in the DDBD method for these reasons: simplicity, the ease with which the relations between the hysteretic shape and equivalent damping are obtained, and the familiarity with elastic spectra for design [8]. Further studies, i.e., [8–10], reveal that the EVD obtained by Jacobsen's original method can be inaccurate. The study performed by Kowalsky and Ayers [9] on concrete structures indicated that on average, assessment of nonlinear response with an equivalent linear system defined by an effective period at the maximum response and the EVD defined by Jacobsen's method can yield good results for the majority of the cases. However, this study also showed that the area-based approach may not be capable of predicting the peak response during earthquakes containing large velocity pulses. Grant et al. [10] and Dwairi et al. [8] with two different methodologies, calibrated the EVD for different hysteresis rules. These studies lead to remarkably similar relationships for the EVD for all hysteresis rules (i.e., elastic-perfectly plastic (EPP), bi-linear (BI), takeda "thin" (TT), takeda "fat" (TF), Ramberg-Osgood (RO) and Flag Shaped (FS)) except EPP. Using real records with comparatively short ground motion duration in the first mentioned study as well as implementing artificial records with longer ground motion durations in the second study was expressed as the reason of difference for EPP hysteresis rule. Afterward, Priestley [11] proposed a general form for the EVD according to inherent damping (i.e., 5 percent) and hysteric damping that depends on the ductility demand. Eq. (2) expresses the EVD equation (ξ_{eq}), based on the ductility demand (μ), suggested by Priestley. The value of 5% is considered as inherent damping and the second part of the equation expresses the hysteretic damping which constant α is calculated by considering the appropriate hysteresis rule for the structure under design and its value varies between 0.1 and 0.7.

$$\xi_{eq}=0.05+\alpha\,\frac{\mu\text{-}1}{\mu\pi} \tag{2}$$

Wijesundra et al. [6] developed a method for calculating the EVD for steel concentrically braced frame structures. They used Jacobsen's method which is then corrected for the earthquake excitation using the results of nonlinear time history analyses conducted using real accelerograms. Pennucci et al. [12] as it is described later, correlated the EVD to the nonlinear response of the analyzed SDOF structures. Esmaeil Abadi and Bahar [13] used Jacobsen and Jennings methods to propose the EVD equation for steel moment-resisting frames (MRFs) in DDBD.

As an effective and simple procedure, the equivalent lateral force (ELF) procedure was developed by Ramirez et al. [14]. The ELF procedure can reduce computational efforts for some types of structures equipped with damping devices. ASCE/SEI 7 [15] also permits the use of this procedure to design structures with damping systems. The ELF procedure considered an equivalent SDOF structure instead of a MODF structure, similar to the DDBD method. Sullivan and Lago [16] developed a non-iterative and simplified procedure in the DDBD method for structures equipped with FVDs. Some studies reveal designing steel structures equipped with FVDs according to the proposed method by Sullivan and Lago lead to conservative design (e.g., [17−19]). To overcome the drawback of the conservative design in the DDBD method, modification of the EVD equation can be efficient.

In this study, the EVD of steel MRFs designed according to the ELF procedure provisions is evaluated. For this purpose, modified Jacobsen's method and the approach used in Pennucci et al.'s study are applied to determine the EVD. Then, results of the obtained EVD by the two mentioned approaches are compared with the assumed value for effective damping in the ELF procedure.

2. Brief review of DDBD in Structures Equipped with FVDs

The DDBD method was first proposed by Priestley [20] as an alternative design approach for force-based design. Fig. 2 illustrates the fundamental of the DDBD method. As mentioned before, the DDBD method considers an equivalent SDOF structure instead of a MDOF structure. The main

characteristics of this SDOF structure are, design displacement (Δ_d), yield displacement (Δ_y), ductility demand (μ), EVD (ξ_{eq}) and effective period (T_{eff}).

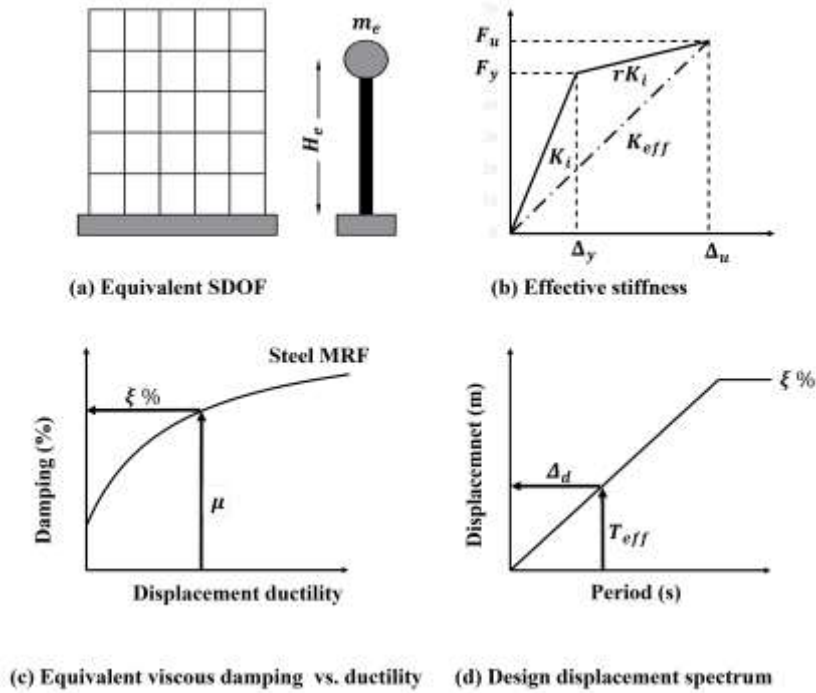(a) Equivalent SDOF

(b) Effective stiffness

(c) Equivalent viscous damping vs. ductility

(d) Design displacement spectrum

Fig. 2. Fundamentals of DDBD

Moreover, the EVD in structures equipped with linear FVDs is determined by:

$$\xi_{eq}=\xi_{el}+\xi_{hyst}+\xi_{FVD} \qquad (3)$$

$$\xi_{FVD}=\frac{\beta}{2} \qquad (4)$$

where ξ_{el} is elastic damping, ξ_{hyst} is hysteric damping that related to post yielding behavior of structure and ξ_{FVD} is the added damping due to linear FVDs and is calculated by Eq. (4) based on the proportion of the design story shear β that should be supported by FVDs on each story. Details and calculations of the mentioned parameters as well as the design procedure are out of the scope of this study and readers can refer to [11, 21].

3. Case Study Structures

In this study, 3-, 6-, and 9-story steel MRFs equipped with linear FVDs are employed to determine the EVD. Two bay width values of 6 m and 8 m for the MRFs were considered. However, the bay width in which FVDs are installed have a constant value of 6 m in all of the case study structures. The heights of stories were considered equal to 3.2 m. The steel MRFs equipped with FVDs are designed for three different percentages of the design base shear, i.e., 0.75, 0.85 and 1.0 in accordance with ASCE/SEI 7. The design ground acceleration of 0.35g (very high seismicity) in accordance with the requirements of the Iranian code of practice for seismic resistant design of buildings, Standard 2800 [22] was considered. All of the case study structures were assumed to be situated on soil type II (i.e., average shear wave velocity to a depth of 30 m would be within the range of 360–760 m/s).

Fig. 3 presents plan views of structures, perimeter MRFs. The diagonal configuration of FVDs is shown in Fig. 4. All columns other than those in the four perimeter MRFs were modeled to only transfer the gravity loads. The dead load was considered equal to 400 kg/m^2. Live loads of 200 and 150 kg/m^2 were considered for floors and roof, respectively. The dead load of the exterior cladding and partition loads were assumed 75 and 100 kg/m^2, respectively.
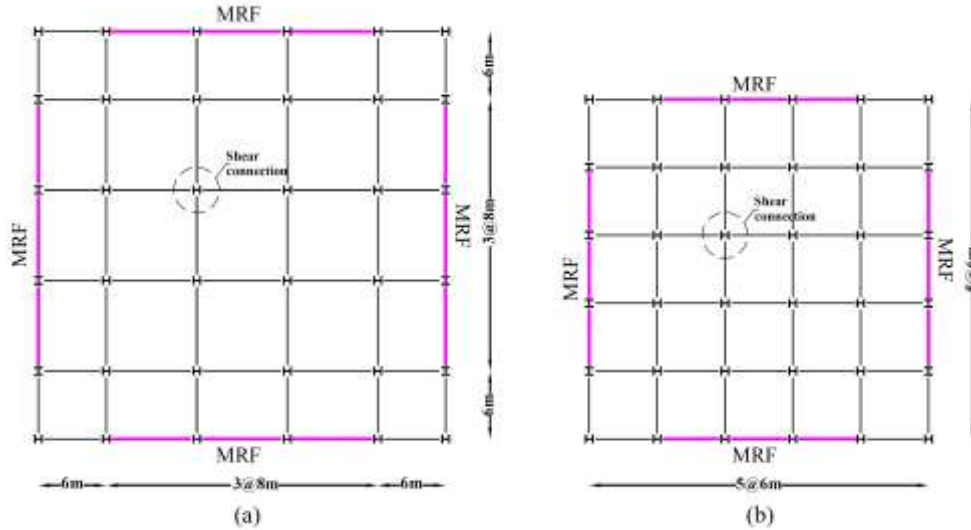

Fig. 3. Plan views of the structures with (a) 8m bays, (b) 6m bays for MRFs
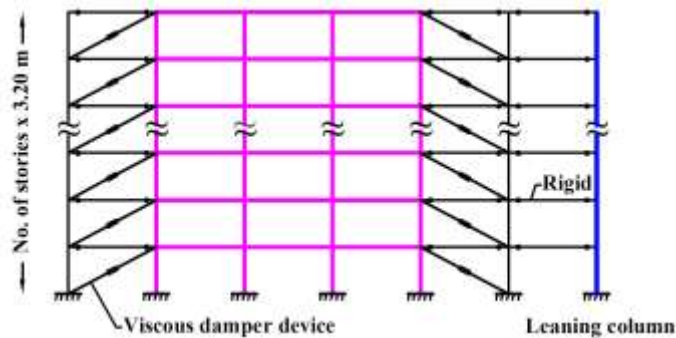
Fig. 4. Diagonal configuration of FVDs

The sum of the dead load and 20% of the live loads was considered as the effective seismic mass of the structures. IPE and IPB shaped sections were used for beams and columns, respectively. The St37-grade steel (with a yield stress of 2400 kg/cm^2) was applied as the material of the structural elements.

4. Numerical Analyses

According to ASCE/SEI 7, seven ground motion records were selected from the pacific earthquake engineering research (PEER) database [23]. The records do not have near-fault pulses and are classified as far-field records. They were recorded at sites with shear wave velocity within the range of 400–750 m/s. The pseudo-spectral acceleration amplitudes of the records were adjusted such that the average of them matches the design response spectrum of Standard 2800 in the period range of 0.0–5.0 seconds. The details of the original records and the corresponding scaling factors are presented in Table 1. Fig. 5 shows the scaled response pseudo acceleration spectra of the records, their average acceleration response spectrum, and the design earthquake (DE) response spectrum. It can be seen that the average spectrum closely match the design spectrum.

Nonlinear time-history analyses (NTHAs) and performance evaluations were performed by SAP2000 program [24] based on two dimensional (2D) models. Link exponential damper element based on Maxwell model was used to simulate nonlinear behavior of fluid viscous dampers.

Inherent damping for NTHAs was taken equal to 3% using Rayleigh damping model [15]. The gravity load combination and plastic hinge properties were applied in accordance with ASCE/SEI 41 [25]. In the analyses, the P-Δ effects were also considered.

Table 1
Detail of Natural Ground Motions

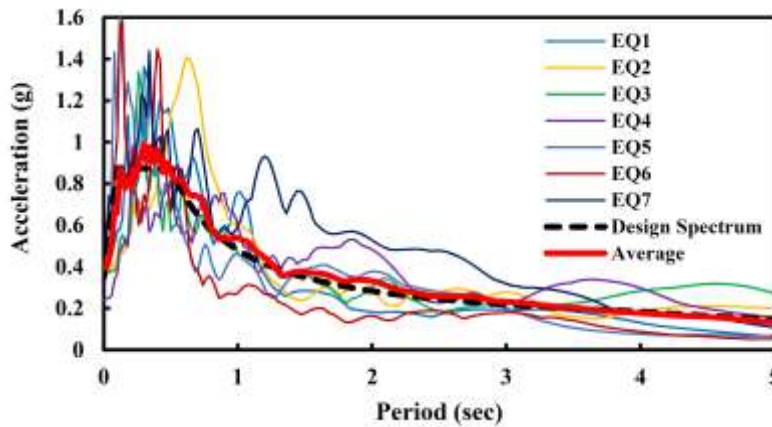| Number	Event	Magnitude	Station	Component	PGA (g)	Scaling factor (DE)
1	Loma Prieta	6.93	Palo Alto - SLAC Lab	360	0.27	1.5061
2	Chi-Chi Taiwan	7.62	CHY029	29N	0.23	1.5379
3	Chi-Chi Taiwan	7.62	TCU042	42N	0.21	1.7282
4	Chi-Chi Taiwan	7.62	TCU116	116N	0.13	1.7473
5	Manjil Iran	7.37	Abbar	Abbar-T	0.49	0.8528
6	Iwate Japan	6.9	Yuzawa	1EW	0.19	2.1521
7	Iwate Japan	6.9	Yuzawa Town	61EW	0.19	2.6255

Fig. 5. Average of pseudo acceleration spectra and design spectrum

5. Design Procedure of MRFs Equipped with FVDs

As mentioned earlier, the design of steel MRFs equipped with FVDs was done following ASCE/SEI 7. At first, with equivalent lateral force (ELF) procedure primary required parameters were obtained and then, NTHAs were performed to confirm or revise the parameters. Similar to Kitayama and Constantinou [26], the following iterative approach was employed to design the frames with dampers as:

Step 1- Design steel MRFs for seismic design base shear equal to 0.75V, 0.85V and 1.00V in the elastic model as a conventional frame with considering seismic provisions (e.g., the weak-beam/strong-column criterion) but without any inter-story drift ratio (IDR) limitations.

Step 2- Calculate damper constant (C) based on the ELF procedure so that the base shear would be equal to 0.75V, 0.85V, or 1.0V. It is important to emphasize that all the FVDs in the present study

were considered linear and the distribution of viscous damping coefficients along the height of the MRFs are uniform.

Step 3- Perform pushover analysis by lateral loads proportional to the first mode of the frames and idealize bilinear curve by ASCE/SEI 7 method. Then, compare base shear strength (V_y) with the design base shear strength calculated in the ELF procedure. Fig. 3 presents pushover curves obtained for the designed frames.

Step 4- If two base shear strengths are not approximately the same, change the sections and iterate steps 1–3 to converge.

Step 5- Conduct NTHAs under the scaled MCE ground motion records. If the IDR is approximately equal to or less than the allowable values in the criteria ASCE/SEI 7, accept the initial assumed damper coefficient calculated by the ELF procedure, else increase the damper coefficient and perform NTHAs until the IDR criterion be satisfied.

For more information and details about the ELF procedure used for the design of the MRFs, the reader is referred to MCEER report by Ramirez et al. [14] and Smart structures by Cheng et al. [27].

Table 2
Some Basic Properties, Damping System Parameters and Average IDRs Obtained from NTHAs for 6m bay Lengths Structures

Model	Period (sec)	V_y (ton) Push over	ELF	Added effective damping ratio (%)	C [ton(s/m)]	Average IDR (%) MCE	DBE
375-6	1.23	115.37	115.19	14.90	94.8555	3.00	1.66
375-6-HP	1.23	115.37	115.19	21.00	133.3120	2.48	1.45
385-6-HP	1.13	128.38	128.97	12.52	83.4041	2.40	1.56
3100-6-HP	1.03	152.53	153.33	9.19	67.8331	2.49	1.60
675-6	1.99	134.10	133.99	16.44	231.7326	2.61	1.66
675HP-6	1.99	134.10	133.99	19.00	267.8175	2.47	1.58
685-6-HP	1.85	148.55	149.01	14.51	209.7912	2.40	1.55
6100-6-HP	1.71	163.94	164.24	12.27	177.5977	2.35	1.70
975-6	2.61	147.8	148.4	17.64	389.7655	2.82	1.69
975-6-HP	2.61	147.8	148.4	25.00	552.3888	2.50	1.46
985-6	2.46	162.75	162.23	15.52	358.3188	2.64	1.60
985-6-HP	2.46	162.75	162.23	17.50	404.0321	2.50	1.51
9100-6	2.29	191.43	190.83	11.66	284.0418	2.67	1.55
9100-6-HP	2.29	191.43	190.83	14.50	353.2252	2.47	1.45

In this study, all of the structures equipped with FVDs were met the IDR of less than 3% at the MCE hazard level. In addition, to have structures with enhanced performance (other than the above-mentioned frames), the IDR was limited to 2.5% at the MCE level. The prefix HP was used to name structures with up to the IDR value of 2.5%. Finally, the fundamental period of the designed structures, comparison of the base shear strengths in the ELF procedure and pushover analyses, added effective damping, damper constants and the obtained average IDRs in NTHAs at the DE and MCE hazard levels under scaled ground motion records were shown in Table 2 and Table 3 for the 6 m and 8 m bay widths structures, respectively. Note that in the names of the structures, the first number indicates the number of stories, the next numbers describe the percentage of calculated using the ELF procedure equations at the DE and MCE hazard levels separately.

base shear that the structure was designed for that, and the number after the dash line defines the bay width of the structure. Table 4 lists the cross-sections for the beams and the columns used in 6 m and 8 m bay widths structures.

6. Methodologies to Obtain EVD and Results

In order to determine the EVD of structures designed as described in section 5, two different methodologies were implemented. Applying modified Jacobsen's method and the approach used in Pennucci et al.'s study. Modified Jacobsen's method was done with the following steps:
Step 1- obtain the average roof displacement from NTHAs under ground motion records.
Step 2- Conduct a NTHA under sinusoidal accelerograms loading with the effective period and arbitrary amplitude. Note that, effective period was

Step 3- Use iteration for the amplitude of sinusoidal accelerograms to converge obtained roof displacements in both NTHAs.

Step 4- Calculate the area of a complete hysteresis loop from sinusoidal loading.

Step 5- Calculate the EVD by using Eq. (1).

Table 3
Some Basic Properties, Damping System Parameters and Average IDRs Obtained from NTHAs for 8m bay Lengths Structures

| Model | Period (sec) | V_y (ton) | | Added effective damping ratio (%) | C [ton(s/m)] | Average IDR (%) | |
		Push over	ELF			MCE	DBE
375-8	1.25	159.70	158.96	14.65	124.3975	3.23	1.69
375-8-HP	1.25	159.70	158.96	22.50	191.0542	2.47	1.47
385-8-HP	1.14	177.20	177.45	12.62	111.6067	2.53	1.51
3100-8-HP	1.01	217.02	216.06	9.82	101.5176	2.41	1.53
675-8	2.09	180.15	181.44	16.53	300.3249	2.84	1.82
675HP-8	2.09	180.15	181.44	20.00	363.3695	2.53	1.62
685-8	1.91	216.90	217.27	12.92	267.6580	2.73	1.75
685-8-HP	1.91	216.90	217.27	15.70	325.2500	2.51	1.53
6100-8-HP	1.78	236.80	235.20	10.89	223.0178	2.53	1.62
975-8	2.70	209.30	208.34	17.03	524.0327	2.90	2.02
975-8-HP	2.70	209.30	208.34	26.50	815.4355	2.50	1.65
985-8	2.56	224.65	225.56	14.92	471.7414	2.72	1.63
985-8-HP	2.56	224.65	225.56	18.50	584.9340	2.54	1.49
9100-8	2.29	279.65	280.16	10.77	399.2498	2.62	1.64
9100-8-HP	2.29	279.65	280.16	13.50	500.4524	2.41	1.53

Table 4
Cross-Sections Obtained According to the ELF Procedure for Case Study Structures

Model	Beams(story)-IPE MRF columns(story)-IPB Corner columns(story)-IPB	Model	Beams(story)-IPE MRF columns(story)-IPB Corner columns(story)-IPB
375-6	400(1-2), 300(3) 320(1-3) 240(1-3)	375-8	450(1-2), 330(3) 400(1-3) 320(1-3)
385-6	400(1-2), 300(3) 360(1-3) 300(1-3)	385-8	500(1), 450(2), 330(3) 450(1-3) 280(1-3)
3100-6	450(1-2), 300(3) 360(1-3) 320(1-3)	3100-8	500(1-2), 360(3) 500(1-3) 340(1-3)
675-6	450(1-4), 400(5), 270(6) 450(1-3), 360(4-6) 340(1-3), 300(4-6)	675-8	550(1-2), 500(3-4), 400(5), 330(6) 500(1-6) 360(1-3), 280(4-6)
685-6	500(1-2), 450(3-4), 400(5), 270(6) 450(1-3), 400(4-6) 400(1-3), 360(4-6)	685-8	550(1-4), 450(5), 330(6) 550(1-3), 500(4-6) 360(1-3), 280(4-6)
6100-6	550(1-2), 500(3), 450(4), 400(5), 270(6) 500(1-3), 400(4-6) 450(1-3), 360(4-6)	6100-8	600(1-2), 550(3-4), 450(5), 330(6) 600(1-3), 500(4-6) 360(1-3), 280(4-6)
975-6	500(1-5), 450(6), 400(7-8), 240(9) 550(1-3), 500(4-6), 340(7-9) 450(1-6), 300(7-9)	975-8	600(1-2), 550(3-6), 500(7), 450(8), 270(9) 650(1-6), 450(7-9) 500(1-6), 400(7-9)

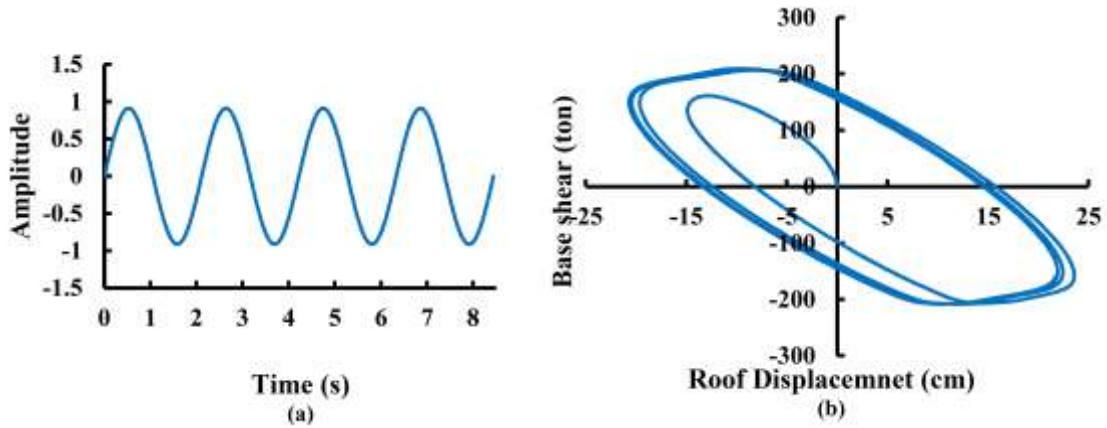| 985-6	550(1-3), 500(4-5), 450(6-7), 400(8). 270(9)	985-8	600(1-4), 550(5), 500(6-8), 270(9)
	550(1-3), 500(4-6), 360(7-9)		700(1-6), 450(7-9)
	400(1-6), 280(7-9)		500(1-3), 450(4-6), 400(7-9)
9100-6	550(1-5), 500(6), 450(7), 400(8), 270(9)	9100-8	750(1), 600(2-7), 500(8), 270 (9)
	600(1-3), 550(4-6), 360(7-9)		800(1-3), 700(4-6), 550(7-9)
	400(1-6), 280(7-9)		500(1-3), 450(4-6), 360(7-9)

Fig. 6. (a) Sinusoidal excitation, (b) Hysteresis curve of sample structure 685-6-HP

As an instance, Fig. 6 (a), shows sinusoidal accelerograms loading that conduced for 685-6-HP structure and Fig. 6 (b), presents the hysteresis curve of the mentioned structure.

Another methodology (i.e., Pennucci et al.) was used in this study includes the following steps:

Step 1- obtain the roof displacements from NTHAs under each ground motion records separately.

Step 2- determine the ductility demand for each record via calculated yield displacement in the ELF procedure.

Step 3- calculate the effective period based on the ELF procedure equation.

Step 4- Convert the roof displacements of the MDOF structures into the SDOF displacements by using the first mode participation factor (Γ_1) for each record.

Step 5- By knowing the displacement of the SDOF structure and effective period, the EVD can be read from the displacement spectrum.

Fig. 7 represents the second methodology procedure used to determine the EVD.

(a) MDOF structure   (b) Calculating roof displacement and ductility   (c) Determine EVD

T_1, D_Y, Γ_1 $\Delta_{SDOF} = \frac{\Delta_{MDOF}}{\Gamma_1}, \mu = \frac{\Delta_{MDOF}}{D_Y}$ $T_{eff} = T_1 \sqrt{\mu}$
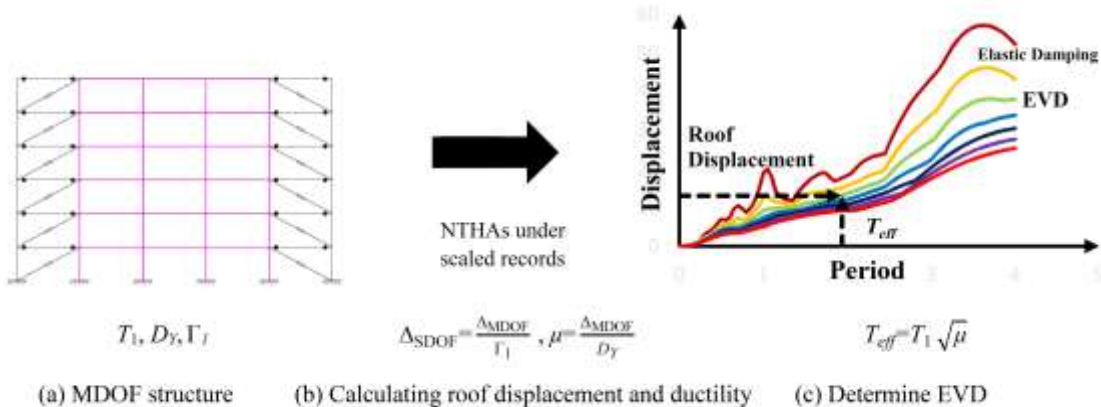
Fig. 7. Determination of EVD based on Pennucci et al.'s Study

7. Results of NTHAs for Determining the EVD

The obtained values of the EVD according to the mentioned methodologies described in the previous section are presented here. Also, these obtained values are compared with values of the EVD based on the ELF procedure calculations. Moreover, verification of the EVD equation proposed by the ELF procedure is investigated.

Fig 8 shows a typical comparison of the obtained EVD results using modified Jacobsen's method Pennucci et al.'s approach and the ELF procedure for the case study structures at the DE and MCE hazard levels. As it can be observed, by considering Pennucci et al.'s approach as an accurate method, modified Jacobsen's method leads to higher values of the EVD in the most case study structures at the DE level.
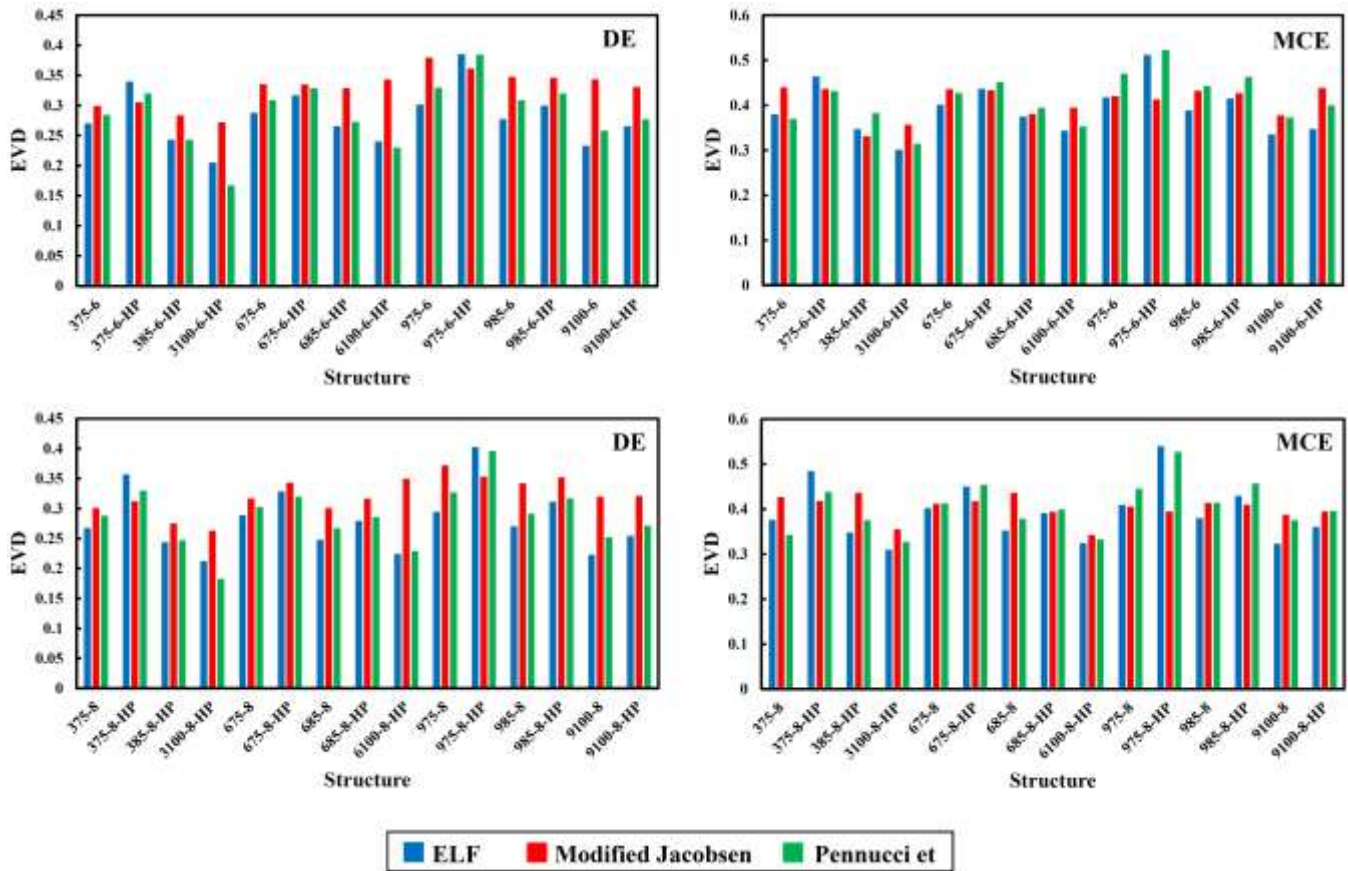

Fig. 8. Comparison of the obtained EVD using different methods for case study structures at DE and MCE levels.

However, unlike the DE level, the EVD obtained by modified Jacobsen's method has lower values at the MCE level. It is worth mentioning that, the obtained values for the EVD in the three approaches (i.e., Jacobsen, modified Jacobsen and Pennucci et al.) are approximately similar for structures with six and eight-meter bays at both the DE and MCE hazard levels. Therefore, it can be shown that the required value of added damping ratio by FVDs can be acceptably obtained by represented values in Table 2 or Table 3 for mid-height steel MRFs structures with different percentages of the design base shears. Also,

these values can help designers to have a rational assumption for the value of added damping ratio by FVDs at the first step of the design according to the ELF procedure. For a better comparison between the three mentioned approaches, Fig. 9 is presented. Fig. 9 (a) depicts the scatter of obtained EVD using modified Jacobsen's method compared with Pennucci et al.'s approach as well as the Fig 9 (b) shows the scatter of the obtained EVD values using the ELF method versus the values obtained from the Pennucci et al.'s approach.

According to Fig. 9 (a), the difference between the obtained EVD values using Pennucci et al.'s approach and those obtained from modified Jacobsen's method is obvious, even though the obtained EVD values obtained from the ELF procedure is significantly matched with the results obtained from Pennucci et al.'s approach, as shown

in Fig. 9 (b). Thus, an acceptable estimation of the ELF procedure to determine the EVD in steel MRF equipped with FVDs is verified. Based on the obtained results for the EVD and ductility demand (μ) in accordance with Pennucci et al.'s approach as well as the added damping ratio related to the FVDs.
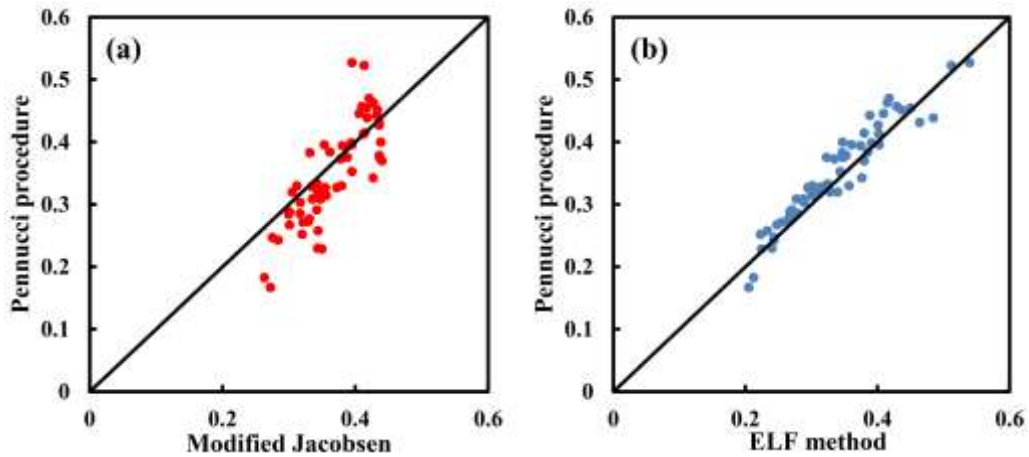
Fig. 9. Comparison between the obtained EVD values using Pennucci et al.'s approach and the corresponding values obtained from the (a) modified Jacobsen's method, (b) the ELF procedure

Fig. 10. Fitted Curve Via Eq. (5) for the EVD Based on the Ductility Demand and Added Damping Ratio, Calculated by MATLAB

$$\text{EVD}=a+b\times\text{FVD}\sqrt{\mu}+c\times(\frac{\mu-1}{\mu\times\pi}) \tag{5}$$

Fig. 10 presents the fitted curve among these three parameters according to the proposed equation as below:

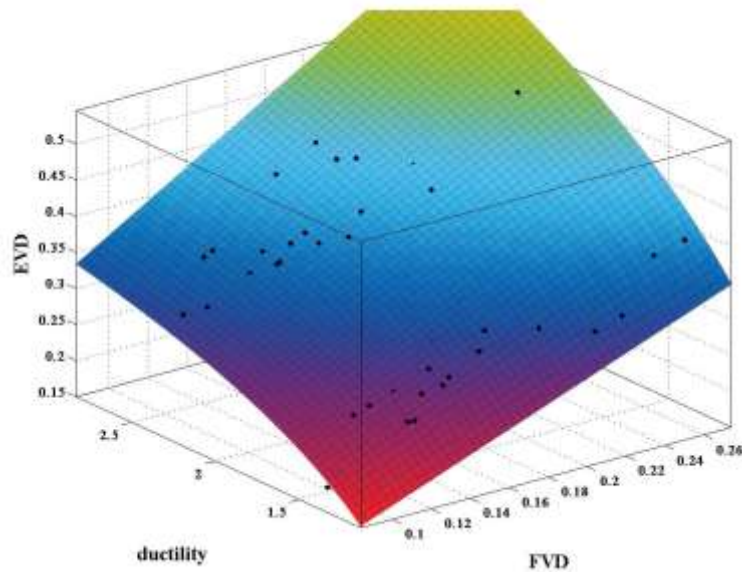where constants *a*, *b* and *c*, are calculated by MATLAB software [28] equal to 0.03671, 0.9644 and 0.7841, respectively. Note that, the general format of Eq. (5) was selected according to the proposed equation by the ELF procedure for calculating effective damping in ASCE/SEI 7. In this regard, constant *a* represents the corresponding value of inherent damping and assumed 0.03 in the ELF procedure. Moreover, constant *b* explained the interaction of ductility demand and added damping ratio in the ELF procedure. Furthermore, based on Eq. (2) the value of α=0.71 was suggested by Pinnucci et al. [29] for determining the hysteretic damping. Finally, a slight difference between the calculated constants by MATLAB and the described constants in the above, verifies the acceptable estimation of the ELF equation for the effective damping in another way.

8. Conclusions

This paper focused on the determination of the EVD for steel structures equipped with linear FVDs which are applied by the ELF equation for calculating the effective damping. For this purpose, two different methods, i.e., modified Jacobsen's method and the approach used in Pennucci et al.'s study were implemented to evaluate the EVD at two seismic hazard levels: the MCE and DE. Based on the extensive NTHAs the following results are obtained:

1- Underestimation of the EVD was resulted via modified Jacobsen's method at the DE hazard level whereas, overestimation of the EVD was seen at the MCE level.

2- Estimation of the EVD by using the ELF procedure that was proposed for calculating the effective damping, was acceptably matched with the results obtained by Pennucci et al.'s approach at both the DE and MCE hazard levels.

3- To estimate the hysteretic damping in steel structures equipped with linear FVDs in the DDBD method, Eq. (3) can be used by considering α =0.71.

4- Considering the interaction of the ductility demand and added damping corresponding to FVDs to estimate the EVD may be improved the design of mid-rise steel structures equipped with linear FVDs in the DDBD method. Further studies are suggested in this case.

References

[1] Yakhchalian M., Asgarkhani N., Yakhchalian M., "Evaluation of deflection amplification factor for steel buckling restrained braced frames", Journal of Building Engineering; 2020, 30, 101228. https://doi.org/10.1016/j.jobe.2020.101228

[2] Gulkan P., Sozen M., "Inelastic response of reinforced concrete structures to earthquake motions", ACI J; 1974, 71(12), 604–610.

[3] Shibata A., Sozen M., "Substitute structure method for seismic design in reinforced concrete", Journal of Structural Division ASCE; 1976, 102(ST1), 1–18.

[4] Jacobsen, L.S., "Steady forced vibration as influenced by damping", Transactions of ASME; 1930, 52, 169–181.

[5] Jacobsen, L.S., "Damping in composite structures" Proc., 2nd World Conf. on Earthquake Engineering; 1960, Vol. 2, Science Council of Japan, Tokyo, 1029–1044.

[6] Wijesundara, K.K., Nascimbene, R., Sullivan, T.J., "Equivalent viscous damping for steel concentrically braced frame structures", Bull Earthquake Eng; 2011, 9, 1535–1558. https://doi.org/10.1007/s10518-011-9272-4

[7] Rosenblueth, E., Herrera, I., "On a kind of hysteretic damping", ASCE Journal of Engineering Mechanics; 1964, 90(4), 37–48.

[8] Dwairi, H.M., Kowalsky, M.J., Nau, J.M., "Equivalent damping in support of direct displacement-based design", Journal of Earthquake Engineering; 2007, 11(4), 512–530. http://dx.doi.org/10.1080/13632460601033884

[9] Kowalsky, M.J., Ayers, J.P., "Investigation of equivalent viscous damping for direct displacement-based design", The Third US-Japan Workshop on Performance-Based Earthquake Engineering Methodology for Reinforced Concrete Building Structures; 16–18 August 2001, Seattle, Washington, Berkeley: Pacific Earthquake Engineering Research Center, University of California, 173–185.

[10] Grant, D.N., Blandon, C.A., Priestley, M.J.N., "Modelling inelastic response in direct displacement-based design", Report 2005/03, IUSS Press, Pavia; 2005.

[11] Priestley, M.J.N., Calvi, G.M., Kowalsky, M.J., "Displacement-Based Design of Structures", IUSS Press, Pavia; 2007.

[12] Pennucci, D., Sullivan, T.J., Calvi, G.M., "Displacement Reduction Factors for the Design of Medium and Long Period Structures", Journal of Earthquake Engineering; 2011, 15:S1, 1–29. http://dx.doi.org/10.1080/13632469.2011.562073

[13] Abadi, R.E., Bahar, O., "Investigation of the LS level hysteretic damping capacity of steel MR frames' needs for the direct displacement-based design method", KSCE J. Civil Eng; 2018, 22, 1304–1315. https://doi.org/10.1007/s12205-017-1321-3

[14] Ramirez, O.M, Constantinou, M.C, Kircher, C.A., Whittaker, A.S., Johnson, M.W., Gomez, J.D., Chrysostomou, C.Z., "Development and evaluation of simplified procedures for analysis and design of buildings with passive energy dissipation systems", Report No: MCEER-00-0010 Multidisciplinary Center for Earthquake Engineering Research (MCEER), University of New York at Buffalo, NY.; 2001.

[15] ASCE/SEI 7-16. Minimum design loads for buildings and other structures, Reston (Virginia): American Society of Civil Engineers; 2017.

[16] Sullivan, T.J., Lago, A., "Towards a simplified Direct DBD procedure for the seismic design of moment resisting frames with viscous dampers", Engineering Structures; 2012, 35, 140-148. https://doi.org/10.1016/j.engstruct.2011.11.010

[17] Noruzvand, M., Mohebbi, M., Shakeri, K., "Modified direct displacement-based design approach for structures equipped with fluid viscous damper", Struct Control Health Monit; 2019, 27(1). https://doi.org/10.1002/stc.2465

[18] Moradpour, S., Dehestani, M., "Optimal DDBD procedure for designing steel structures with nonlinear fluid viscous dampers", Structures; 2019, Volume 22, 154–174. https://doi.org/10.1016/j.istruc.2019.08.005

[19] Alehojjat, S.B., Bahar, O., Yakhchalian, M., "Improvements in the direct displacement-based design procedure for mid-rise steel MRFs equipped with viscous dampers", Structures; 2021, Vol. 34, 1636–1650. https://doi.org/10.1016/j.istruc.2021.08.047

[20] Priestley, M.J.N., "Myths and fallacies in earthquake engineering conflicts between design and reality", Bulletin of the New Zealand National Society for Earthquake Engineering; 1993, Vol. 26(3), 329–341.

[21] Sullivan, T.J., Priestley, M.J.N., Calvi, G.M., "A Model Code for the Displacement-Based Seismic Design of Structures (DBD12)", IUSS Press, Pavia; 2007. ISBN: 978-88-6198-072-3.

[22] Standard No. 2800. Iranian Code of Practice for Seismic Resistant Design of Buildings, Standard No. 2800, 4th edition, BHRC Publication No. S-253, Iran, Tehran; 2014.

[23] PEER, PEER NGA database, Pacific Earthquake Engineering Research, Univ. of California, Berkeley, CA.; 2005. https://ngawest2.berkeley.edu/

[24] CSI, SAP2000, Integrated Software for Structural Analysis and Design, Computers and Structures Inc., Berkelely, California; 2018.

[25] ASCE/SEI 41-13. Seismic Evaluation and Retrofit of Existing Buildings, ASCE/SEI 41, Reston, (Virginia): American Society of Civil Engineers; 2014.

[26] Kitayama, S., Constantinou, M.C., "Seismic performance of buildings with viscous damping systems designed by the procedures of ASCE/SEI 7-16", Journal of Structural Engineering; 2018, Vol 144(6). https://doi.org/10.1061/(ASCE)ST.1943-541X.0002048

[27] Cheng, F.Y., Jiang, H., Lou, K., "Smart Structures Innovative Systems for Seismic Response Control", CRC Press; 2008, ISBN: 13:978-0-8493-8532-2.

[28] MATLAB 2014a, The Math Works, Inc., Natick, Massachusetts, United States; 2014.

[29] Pennucci, D., Sullivan, T.J., Calvi, G.M., "Performance Based Design of Tall RC Wall Buildings", ROSE Research Report 2011/02; IUSS Press, Pavia; 2011.